Epitope mapping of Ebola virus dominant and subdominant glycoprotein epitopes facilitates construction of an epitope-based DNA vaccine able to focus the antibody response in mice

Daniel A.J. Mitchell[1], Lesley C. Dupuy[1], Mariano Sanchez-Lockhart[1], Gustavo Palacios[1], Jaap W. Back[2], Katya Shimanovskaya[2], Sidhartha Chaudhury[3], Daniel R. Ripoll[3], Anders Wallqvist[3], and Connie S. Schmaljohn[1]

[1]United States Army Medical Research Institute of Infectious Diseases (USAMRIID), Fort Detrick, MD, USA

[2]Pepscan Presto BV, Lelystad, the Netherlands

[3]Biotechnology HPC Software Applications Institute, Telemedicine and Advanced Technology Research Center, US Army Medical Research and Materiel Command, Fort Detrick, MD, USA

Abstract

We performed epitope mapping studies on the major surface glycoprotein (GP) of Ebola virus (EBOV) using Chemically **Li**nked Peptides on Scaffolds (CLIPS), which form linear and potential conformational epitopes. This method identified monoclonal antibody epitopes and predicted additional epitopes recognized by antibodies in polyclonal sera from animals experimentally vaccinated against or infected with EBOV. Using the information obtained along with structural modeling to predict epitope accessibility, we then constructed two DNA vaccines encoding immunodominant and subdominant epitopes predicted to be accessible on EBOV GP. Although a construct designed to produce a membrane-bound oligopeptide was poorly immunogenic, a construct generating a secreted oligopeptide elicited strong antibody responses in mice. When this construct was administered as a boost to a DNA vaccine expressing the complete EBOV GP gene, the resultant antibody response was focused largely toward the less immunodominant epitopes in the oligopeptide. Taken together, the results of this work suggest a utility for this method for immune focusing of antibody responses elicited by vaccination.

Introduction

Ebola virus (EBOV) causes severe hemorrhagic fever with a mortality rate as high as 90%. The recent outbreak in West Africa resulted in renewed efforts to develop efficacious recombinant DNA-based vaccines, most of which are based on eliciting immune responses to the major surface glycoprotein (GP) of EBOV. We previously reported the development and animal testing of filovirus DNA vaccines expressing full length GP genes [1-3]. Similar to protein and whole-virus vaccination, the expression products of the DNA vaccines present a multitude of epitopes to the host immune system, many of which do not confer protective immunity. Since immunodominant epitopes are those that offer the most favorable accessibility and binding kinetics to antibodies, the immune response is skewed toward them. This phenomenon has been observed for other pathogens, with the best example being influenza. In this case, the influenza hemagglutinin 1 (HA1) globule undergoes rapid evolution under immune pressure generating poorly cross-protective immunodominant epitopes that can serve as immunological decoys [4].

Here, we sought to determine if it is possible to overcome immunodominance using a defined multi-epitope DNA vaccine construct expressing both immunodominant and subdominant gene regions. Toward this goal, we conducted a three-part study to select and test the immunogenicity of DNA vaccine constructs encoding both immunodominant and subdominant epitopes. First, we performed epitope mapping studies using Chemically Linked Peptides on Scaffolds (CLIPS), which are able to form both linear and conformational epitopes [5]. We screened EBOV-specific monoclonal antibodies (MAbs), which recognize immunodominant epitopes. We next screened polyclonal sera from mice, guinea pigs and nonhuman primates

(NHP) experimentally vaccinated against or infected with EBOV in an attempt to identify less immunodominant epitopes. Finally, we selected a subset of these epitopes to design two minimal epitope-based DNA vaccines. We show here that not only can such a construct focus a humoral immune response, but immunodominance can be overcome due to epitope availability within the construct.

Results

CLIPS libraries

A general description of CLIPS technology and types of scaffolds used in screenings has been described previously[5]. A total of 7,286 different CLIPS peptides derived from the EBOV GP-1 and GP-2 amino sequences were synthesized on scaffolds and placed into 14 different groups for screening. Group 1 included overlapping looped 15-mers, and Group 2 comprised overlapping linear 15-mers. The remaining groups consisted of 21-mer or 32-mer peptides constructed from 9-mers separated by two cysteine residues and additional terminal cysteine residues to allow disulfide bond formation. Each 9-mer in the sequence was paired with sequential 9-mers across the GP amino acid sequence resulting in a peptide library that was intended to simulate both linear and conformational epitopes [5]. For fine mapping of specific antigenic regions of EBOV GP, a series of 6,518 additional CLIPS peptides were generated based on the initially retrieved leads. These fine mapping variants include all proteogenic amino acid substitutions at each amino acid position within putative epitopes to allow assessment of the individual residue contributions to the epitopes.

Epitope mapping with mouse antibodies

The CLIPS libraries were probed with mouse mAbs 13F6, 13C6, 6D8 and 6E3[6] and with sera from experimentally vaccinated or infected mice, guinea pigs, and rhesus macaques. Initial screening showed that mAb 13F6 binds to peptides in groups 1, 2, 7, and 13 **(Figure S1).** Full substitution mutagenesis revealed clear binding to $_{391}$TPVYKLDISEATQVEQHHRRTDNDS$_{415}$ and indicated that the amino acids $_{406}$QHHRRTD$_{412}$ are the core of the epitope, with the motif $_{406}$QXXRXT$_{411}$ being most essential **(Figure 1A)**. Similarly, mAb 6E3, which was previously found to be in the same competition group as mAb 13F6[6], bound to this same region, and full substitution mutagenesis revealed that the core of the epitope was $_{406}$QHHRRTD$_{412}$ with $_{406}$QXHRR$_{410}$ as the most important residues (**Figure 1B)**. The mAb 6D8 also bound to CLIPS peptides having the amino acid sequence $_{391}$TPVYKLDISEATQVEQHHRRTDNDS$_{415}$, and full substitution mutagenesis showed that $_{394}$YKLDI$_{398}$, was the core of the epitope with $_{395}$KLD$_{397}$ as the most essential amino acids **(Figure 1C)**.

Control sera from naïve mice or mice vaccinated with an empty vector DNA vaccine showed no binding in the CLIPS screening (data not shown). Screening of pooled sera from mice vaccinated with a wild-type (WT) EBOV GP DNA vaccine revealed binding to peptides in groups 1, 2, 3, and 13 (**Figure S2**). For fine mapping using the second CLIPS library, we screened two additional serum pools from mice vaccinated with a codon-optimized WT EBOV GP DNA vaccine, which we found to have improved expression as compared to our non-optimized DNA vaccine[2]. We also screened a sample from mice that were vaccinated with the Venezuelan equine encephalitis virus replicon particle (VRP)-based EBOV GP vaccine that was originally

used to generate the mouse MAbs in this study and that survived challenge with EBOV [6]. As with sera from mice vaccinated with the non-optimized WT GP DNA vaccine (**Figure S2**), sera from mice vaccinated three times with the optimized GP DNA vaccines as well as the sera from the VRP vaccinated and EBOV challenged survivor showed strong binding to $_{391}$TPVYKLDISEATQVEQHHRRTDNDS$_{415}$ (data not shown). Positional scanning using the optimized WT GP DNA-vaccinated mouse sera showed $_{397}$DISEAT$_{402}$ to be the core of the epitope recognized, with $_{398}$ISXXT$_{402}$ as the most crucial amino acids **(Figure 1D)**, while positional scanning of the VRP survivor showed $_{395}$KLDI$_{398}$ as the core of the epitope (data not shown) similar to what was observed for Mab 6D8 (**Figure 1C**). Our data indicate that this region of the mucin-like domain, which also includes the epitope binding regions for mAbs 13F6, 6E3, and 6D8, is highly immunodominant in mice. In addition to this region, we also observed binding by the polyclonal WT GP DNA-vaccinated mice to CLIPS with the amino acids $_{41}$STLQVSDVDKLVCRDKLLSSTNMLRS$_{65}$ and peptides containing $_{197}$HPLREPVNATED$_{206}$ (data not shown).

Our initial screening with mAb 13C6 showed binding to CLIPS peptides in Groups 1, 2, 7, 12, and 13 (**Figure S3)**. The mAb 13C6 epitope is conformational and binds to both GP1 and sGP[6]. The epitope for this mAb has been reported to reside in the glycan cap region of GP1, a region containing six N-linked glycosylation sites, which is believed to shield the receptor binding domain[7-9]. Our CLIPS binding results are inconsistent with this finding, and instead show binding to a region near epitopes for mAbs 12B5[6] and 14G7[6]. We repeated the experiment using a different aliquot of mAb 13C6, which was derived from a separate hybridoma subclone, with the same results. We also compared the productive IG-H rearranged

nucleotide sequences from the two clonal derivatives (13C6 1.1 and 13C61.1.1) and found them to be identical to one another and to the original reported nucleotide sequences for 13C6 (data not shown). To further investigate our findings with mAb 13C6, we generated phage libraries displaying WT EBOV GP peptides as described previously[10]. This library was constructed to display 50-mer long peptides from EBOV GP at the end of the T7 capsid, with a sliding window of 10 amino acids from the previous peptide. Panning with mAb 13C6 enriched phages displaying $_{461}$NNNTHHQDTGEESASSGKLGLITNTIAGVA GLITGGRRTR$_{500}$ peptide, which includes the same region (underlined) identified with CLIPS. This region also includes the epitope for mouse mAbs 12B5 and 14G7[6, 11].

To explore the residues that contribute most to the mAb 13C6 binding, we performed positional scanning with mAb 13C6 in comparison to mAb 6D8. As expected, mAb 6D8 bound to $_{391}$TPVYKLDISEATQVEQHHRRTDNDS$_{415}$, and substitutions for residues $_{394}$YKLDI$_{398}$ negatively impacted binding (**Figure 2A**). Also as expected, mAb 6D8 did not bind to the $_{470}$GEESASSGKLGLITNTIAGVAGLIT$_{493}$ region identified for mAb 13C6 binding (**Figure 2B**). Conversely, mAb 13C6 bound poorly to the mAb 6D8 epitope $_{391}$TPVYKLDISEATQVEQHHRRTDNDS$_{415}$ (**Figure 2C**), but bound strongly to $_{470}$GEESASSGKLGLITNTIAGVAGLIT$_{493}$ (**Figure 2D**). The residues that contribute most to mAb 13C6 binding in this assay are those comprising the motif on the end of this peptide: $_{487}$GxAGLIT$_{493}$. Of note, introduction of a negatively charged residue (D or E) at any point disturbed binding (**Figure 2D**).

Mouse, guinea pig and rhesus macaque polyclonal sera screening

To detect additional EBOV GP epitopes, we screened polyclonal sera from mice or guinea pigs experimentally vaccinated with DNA constructs expressing EBOV GP and with sera from rhesus macaques that survived EBOV infection. Sera tested with the first CLIPS library included negative and positive control samples from mice vaccinated with the empty vector DNA vaccine (**Vector, Figure 3**). In addition to pooled sera from mice vaccinated with a WT EBOV GP DNA vaccine, we also screened pooled sera from mice vaccinated with DNA constructs in which one or the other of the two GP2 N-linked glycosylation sites were mutated as described previously[12]. In our earlier studies, we found that mutating $_{563}$NET$_{565}$ to $_{563}$AET$_{565}$ (**MUTC Figure 3**) resulted in GP2 that did not co-precipitate with GP1 and that had reduced immunogenicity and protective efficacy in mice. In contrast, mutating $_{618}$NIT$_{620}$ to $_{618}$AIT$_{620}$ (**MUTD Figure 3**) resulted in GP2 that still co-precipitated with GP1 and minimally impacted elicitation of protective immunity [12]. Consequently, we reasoned that these sera might recognize different GP epitopes than sera from mice vaccinated with WT EBOV GP DNA vaccines. The two pooled Guinea pig serum samples were from earlier EBOV DNA vaccine studies, with one obtained from Guinea pigs vaccinated with the EBOV GP DNA vaccine (**130**, **Figure 5**) and the other **(107, Figure 5**) from Guinea pigs vaccinated with EBOV GP and NP DNA vaccines (unpublished data). The rhesus macaque samples screened were convalescent samples of survivors of EBOV infection studies[13, 14].

Like samples from mice vaccinated with the WT EBOV GP DNA vaccine (**Figures 1 and S3**), CLIPS screening of pooled sera from mice that had been vaccinated with MUTD DNA

showed strong binding to CLIPS peptides containing $_{391}$TPVYKDLDIS$_{399}$, whereas samples from MUTC vaccinated mice did not (**Figures 3 & S5**). One of the guinea pig samples (**130**, **Figure 3**) and one of the rhesus macaque samples (**C250B**, **Figure 3**) also showed strong binding to this region of GP. Sera from mice vaccinated with MUTC and MUTD, but not with WT GP DNA vaccines, bound strongly to $_{43}$LQVSDVDKLVCRDKL$_{57}$ (**Figure 3**), suggesting that the mutant DNA vaccines were eliciting different antibody responses. This same region was also recognized by one of the guinea pigs samples (**130, Figure 3**). The two guinea pig samples also recognized several epitopes that were not strongly bound by antibodies in the polyclonal mouse sera, but were bound by rhesus macaque sera (**Figure 3**). Only two of the rhesus macaque sera **(R1510 and C250B, Figure 3**) bound strongly to epitopes in GP2, although weaker binding was also noted for mouse and guinea pig samples (**Figure 3**).

Construction of epitope-based DNA vaccines

Using the CLIPS data and structural modeling based on the initial X-ray crystal structure of EBOV GP[15], we sought to determine if it is possible to present the immune system with both immunodominant and subdominant epitopes and generate immune responses to all of them. As representative immunodominant epitopes, we included gene regions encoding the epitopes for mouse mAb 6D8 ($_{392}$PVYKLDISEA$_{401}$), and mAbs 13F6 and 6E3 ($_{406}$QHHRRT$_{411}$). We also included the gene region encoding $_{477}$GKLGLITN$_{484}$, because in CLIPS screening this epitope was recognized strongly by sera from guinea pigs and rhesus macaques (**Figure 3**). Also, this region encodes the amino acids in the two overlapping peptides that were originally shown to be recognized by mouse mAbs 12B5 and 14G7 ($_{477}$GKLGLITNTIAGVAGLI$_{493}$) [6, 11] **(mAb 12B5 (partial), Table1**), as well as in our CLIPS and phage display screenings with mAb 13C6 (**Figures**

2 & S4). Multi-epitope construct 1 (Mep1) was designed to also include two subdominant epitopes that were predicted to be accessible on the surface of EBOV GP (**M1 & M2, Figure 4**), one of which ($_{88}$FRSGVPPK$_{95}$) was weakly recognized in CLIPS screenings using guinea pig and rhesus macaque sera and the other of which ($_{111}$LEIKKPDG$_{118}$) was not recognized by any of the immune sera (**Figure 3**). There was no linker between the signal peptide and the M1 epitope in Mep1, but all of the other epitopes were separated by flexible linkers consisting of four glycine residues (**Table 1).** This construct also included the amino terminal EBOV signal peptide (33 amino acids) preceding the epitopes to facilitate intracellular trafficking. The EBOV transmembrane domain was included to anchor the construct to the cell surface (**Table 1**).

Like Mep1, Mep2 contained the EBOV signal peptide, but differed from Mep1 in that it also encoded the first 7 amino acids of the amino terminus of GP1 (**Table 1**). These 7 amino acids were included to potentially enhance signal peptide removal prior to a glycine linker, which was inserted before each epitope. Mep2 was intended to generate a secretion product it did not have a transmembrane domain. The same three immunodominant epitopes as in Mep1 were included in Mep2, which were followed by two linear epitopes that were predicted to be surface accessible on EBOV virions (**M3 & M4, Figure 4**), but did not appear to be immunodominant in mice vaccinated with the WT EBOV GP DNA vaccine. One of these (M3) is the epitope that was bound by antibodies in sera from mice vaccinated with the two glycosylation mutants and one of the guinea pig pools ($_{45}$VSDVDKLVCRDKL$_{57}$), but not by sera from mice vaccinated with the WT EBOV GP DNA vaccine (**Table 1 & Figure 3**). The other (**M4, Figure 4)** is an epitope recognized by both guinea pig sera and one of the rhesus macaque sera in the CLIPS screen ($_{195}$SSHPLREPV$_{203}$), but was not strongly bound by any of the mouse samples

(**Figure 3**). Mep2 also included two putative conformational epitopes identified by CLIPS screening, each consisting of a simple double-loop structure with the linear, protective, neutralizing epitope of mAb 6D8 followed by two C residues to allow disulfide bonding and one of two overlapping regions from the mucin-like domain ($_{433}$ENTNTSKG$_{441}$ or $_{427}$AGPPKAENT$_{435}$) that were weakly bound by guinea pig and rhesus macaque samples, but not by mouse samples (**Table 1 & Figure 3**). Both Mep constructs produced polypeptides recognized by mAb 6D8 when assayed by immunofluourescent antibody staining of transfected cells (**Figure 5A**). As expected, ELISA of cell culture supernatants from transfected cells demonstrated that Mep2, but not Mep1 produced a secreted expression product (**Figure 5B**). Western blots of a Mep1 cell lysate with mAb 6E3 or Mep2 cell supernatant with mAb 6D8 showed expression products of the expected sizes (data not shown).

Mouse immunogenicity and immune focusing

To evaluate the immunogenicity of the epitope constructs, we vaccinated groups of 10 mice with the Mep1 or Mep2 DNA vaccines three times at 3-week intervals using intramuscular electroporation. Blood samples collected at day 0 and 3 weeks after each vaccination were analyzed by ELISA using whole EBOV antigen. Mep1 elicited no detectable antibody response after two vaccinations and only a low response after three vaccinations. Mep2 elicited a detectable response after two vaccinations with a rise in ELISA antibody titer after three vaccinations (**Figure 5C**). Consequently, to determine if the multi-epitope constructs could influence immunodominance, we used Mep2 to vaccinate mice either alone or as a boost to WT GP. We assessed antibody responses by ELISA using peptides that contained the epitopes of interest (**Table S2**).

Sera from mice vaccinated once with the WT GP DNA vaccine had low antibody responses to peptides corresponding to epitope M4 as well as those recognized by mAbs 6D8 and 13F6 (**Figure 6A**). After three vaccinations with WT GP, additional responses to the other peptides excluding those representing epitope M3 were also detected (**Figure 6B**). In contrast, three vaccinations with Mep2 yielded strong responses to peptides representing M3 and M4, with little response to the other peptides (**Figure 6C**). When mice were vaccinated once with the WT GP DNA vaccine followed by two booster vaccinations with Mep2, strong responses to peptides representing M3 and M4 were observed, as well as a moderate response to peptides representing epitopes for mAbs 6D8, 13F6 and 12B5 (**Figure 6D**). These data suggest that the Mep2 construct is able to skew the immune response of the WT GP DNA vaccine toward subdominant epitopes found in the WT GP construct.

Discussion

In this study, we evaluated epitope-specific antibody responses to EBOV GP using CLIPS libraries probed with mouse mAbs and polyclonal antibody samples from experimentally vaccinated or infected animals. For the mouse mAb 13F6, the residues $_{406}$QXXRXT$_{411}$ were found to be crucial to the core of the epitope, which is in agreement with a recent alanine scanning study that implicated Q406, R409, T411, and D412 as crucial to epitope binding[16]. Likewise, CLIPS screening with mAb 6E3 defined the crucial residues for binding to be QXHRR. This slight difference in the critical binding residues defined for mAbs 6E3 and 13F6 augment earlier findings indicating that they also differ in isotype (IgG1 vs. IgG2a, respectively) and ability to confer passive protection in mice[6]. CLIPS screening and positional mapping of the mAb 6D8 epitope, which identified residues $_{395}$KLD$_{397}$ as critical for binding, agrees with other

studies[6, 16], but further delineates this epitope. In contrast, our results with mAb 13C6 do not correlate with those from earlier structural studies, which clearly show that mAb 13C6 binds to the glycan cap region of EBOV GP[16-19]. In our studies, both CLIPS libraries identified a binding region for mab 13C6 just outside the mucin-like domain and before the furin cleavage site for GP1 and GP2 and in the same region bound by mAbs 12B5 and 14G7[6]. Panning of a phage display library identified the same binding region as the CLIPS libraries, and full mutagenesis scanning corroborated these results and indicated that substitutions to $_{487}$GxAGLIT$_{493}$ negatively correlate with binding. Although we have not determined the reason for the discrepancies between our results and the structural data, of note is that our work was performed using the original mouse mAb 13C6 [6], whereas the structural studies used a chimeric human/mouse mAb produced in plants [19]. Differences in the heavy chains of mouse mAb 4G7 and the analogous chimeric mAb c4G7 were postulated to explain differences in binding observed in structural studies[19]. Alternatively, what we observed could be due to promiscuous binding of mAb 13C6. One possibility is that the CLIPS studies are detecting the peptide $_{475}$SSGKL$_{479}$ rather than $_{270}$TTGKL$_{273}$ in the glycan cap as in the electron microscopy (EM) studies[19]. The T residues in the epitope identified in the EM structure form a tight loop that goes deep in the antibody binding pocket of mAb 13C6. On the other hand, our positional scanning (**Figure 5**) shows that T residues replacing both S residues in $_{475}$SSGKL$_{479}$ are the most unfavorable of the amino acid changes possible. In other words, the conformation of the $_{270}$TTGKL$_{273}$ fragment found in the GP/sGP structure is not a favorable one on the oligopeptides, and the loop in the x-ray structure is probably forced during the folding process of GP. It would be interesting to perform a structural study with mAb 13C6 and these linear epitopes, similar to the study

already reported for mAb 14G7 and its linear peptide epitope, which resides in the same region of the mucin-like domain that we identified for mAb 13C6.

Other interesting, but unsurprising findings from our CLIPS screenings were the differing epitopes recognized by antibodies in polyclonal sera of vaccinated or infected mice, guinea pigs and rhesus macaques. Clearly, the small number of samples that we screened prevent generalizations about immunodominant epitope differences, but they do hint that there are both highly immunodominant epitopes on GP that are frequently recognized by all species tested as well as epitopes that might be more commonly recognized by various specific species or when comparing vaccinated versus infected animal samples.

For the purposes of our work, we chose epitopes recognized by mouse mAbs 6D8, 13F6 and 12B5, but did not include that of mAb 13C6 due to the discordant mapping results, as the immunodominant portions of our constructs. We also selected four accessible, but subdominant epitopes to combine with these to determine if the immunodominant epitopes would obstruct the generation of broad immunity. Although both the Mep1 and Mep2 constructs produced intracellular oligopeptides recognized by IFA with EBOV mAbs, the Mep2 expression appeared to be stronger. More importantly, Mep1 was poorly immunogenic in mice. We suspect the poor immunogenicity of Mep 1 was related to the transmembrane domain, which was intended to allow cell surface presentation of the epitopes. It is possible that this anchoring did not provide adequate presentation to the mouse immune system or that the oligopeptide did not assume a favorable conformational structure to elicit strong antibody responses in mice. Alternatively, cleavage of the signal peptide or intracellular trafficking might have been suboptimal due to the amino acids of the first epitope, which are different from

those of authentic EBOV GP. To eliminate these potentially negative impacts on immunogenicity, we designed our second construct, Mep2, to encode the signal peptide followed by the first 7 amino terminal residues of GP1 and a four glycine linker before the first epitope. We also eliminated the transmembrane coding region to promote secretion of the expression product. Mep2 was found not only to have better intracellular expression than Mep1, but also was secreted and elicited a much better antibody response than Mep1 in vaccinated mice.

To assess the antibody responses to the Mep2 epitopes, we performed ELISA using overlapping linear epitopes. We found the Mep2 construct elicited strong responses to the subdominant epitopes M3 and M4, with weak to no responses to the dominant epitopes. In contract, the WT GP construct elicited stronger responses to the dominant epitopes. When used as a boost to WT GP, the responses skewed to the subdominant epitopes in Mep2. We did not detect antibody responses to two peptides designed as simple double-loop structures including the linear protective epitope of mAb 6D8; however, we do not know if these epitopes folded correctly or were presented effectively to elicit an antibody response.

In conclusion, our data suggest that it is possible to use a multi-epitope DNA vaccine construct to focus the immune response toward desired, accessible epitopes, even in the presence of normally immunodominant epitopes. This has implications for filovirus DNA vaccines that contain epitopes conserved among several viruses, which could be used to boost otherwise subdominant antibody responses.

Methods

Cell lines and virus propagation

COS-7 or Vero E6 cells were cultured in DMEM supplemented with 10% FBS and antibiotics (Penicillin/Streptomycin, 50 U/mL) at 37^{o}C with 5% CO_2. EBOV strain Mayinga was propagated in Vero E6 cells. When cells reached 90% confluency, the culture medium was removed and cells were infected under BSL4 conditions at an MOI of 0.01. After 1 hour, the inoculum was removed and fresh medium was added. The infected cultures were incubated at 37^{o}C with 5% CO_2. Cells were monitored daily for cytopathogenic effects (CPE) and when > 90% of the infected cells had detached from the culture vessel surface, the culture fluids were harvested, clarified by centrifugation and frozen at -80^{o}C.

Plasmids

All plasmid constructs in this study used the pWRG7077 vector described previously[20]. Constructs expressing WT GP or a selection of epitopes from the GP gene were codon-optimized for Homo sapiens and synthesized by GeneArt. Large-scale preparations of purified, research-grade plasmids were produced by Aldevron.

CLIPS peptide libraries

CLIPS libraries were synthesized by Pepscan Systems (The Netherlands). The first library consisted of a total of 7,286 different CLIPS peptides divided into 14 groups to include: (1) All overlapping looped 15-mers, 1-662; (2) All overlapping linear 15-mers, 663-1324; (3) Combi double-looped 21-mers on T3 CLIPS, 1325-1580; (4) Combi triple-looped 32-mers on P2T3 CLIPS, 1581-2309; (5) Combi triple-looped 32-mers on P2T3 CLIPS, 2310-3038; (6) Combi triple-looped 32-mers on P2T3 CLIPS, 3039-3767; (7) Combi triple-looped 32-mers on P2T3 CLIPS,

3768-4279; (8) Combi triple-looped 32-mers on P2T3 CLIPS, 4280-4404; (9) Combi triple-looped 32-mers on P2T3 CLIPS, 4405-4620; (10) Combi triple-looped 32-mers on P2T3 CLIPS, 4621-5132; (11) Combi triple-looped 21-mers on P2T3 CLIPS, 5133-5757; (12) Combi triple-looped 21-mers on P2T3 CLIPS, 5758-6118; (13) Combi triple-looped 21-mers on P2T3 CLIPS, 6119-7142; (14) Combi triple-looped 21-mers on P2T3 CLIPS, 7143-7286 (**Figure S1A**). The second library was synthesized for fine mapping and included 3,750 34-mer CLIPS peptides to include: single-looped peptides on T2 scaffold, double-looped peptides on T3 scaffold, double-looped peptides on T2+T2 scaffold, triple-looped peptides on T2+T3 scaffold and sheet or helix-like peptides on T2+T2 scaffold (**Figure S1B**).

To probe the individual contributions of amino acids at certain positions, full substitution mutagenesis arrays were designed based on the initially retrieved leads. All peptides were synthesized on solid support and screened with varying concentrations of antibody and blocking buffer in order to optimize signal-to-noise ratios in each experiment[5].

Mouse vaccinations with epitope-based DNA vaccines

Plasmid DNA was prepared at 25 µg/20 µl in PBS. Groups of 6-8 week-old female BALB/c mice (N=10) were vaccinated three times at three-week intervals with 20 µl of DNA by intramuscular electroporation. Anesthetized mice were vaccinated in the tibialis anterior muscle using the Ichor Medical Systems Tri-Grid Delivery System[21]. Prior to each vaccination and at week 9, blood was collected and serum was isolated by centrifugation for ELISA.

Immunofluorescence microscopy

COS-7 cells were cultured on 12 mm coverslips in 24-well plates under conditions described above. When cells reached 80% confluency, they were transfected with 1 µg of purified plasmid DNA using Lipofectamine (Life Technologies). Twenty-four hours after transfection, medium was removed and the cells were washed with PBS and then fixed with 10% formalin. Cells were then permeabilized with PBS + 0.1% Triton-X for 5 minutes, washed with PBS, and blocked with PBS + 1% Tween 20 + 5% nonfat dried milk (NFDM). Next, cells were washed and incubated with mAb 6D8 (generously provided by John Dye, Jr.) for 1 hr. Finally, cells were washed, incubated with Alexa Fluor 488 goat anti-mouse IgG for 30 minutes, washed again, mounted onto slides with ProLong Gold Antifade reagent (Life Technologies) and imaged by fluorescence microscopy.

Immunoblotting

COS-7 cells were transfected with plasmid DNA encoding WT GP, the multi-epitope construct, or empty vector. Cells were harvested, lysed in RIPA buffer and resolved on SDS-PAGE followed by transfer to PVDF for western blot. Western blotting was performed as per manufacturer's instructions using the Novex WesternBreeze Immunodetection kit. Primary antibody for these blots was mAb 6D8. Blots were blocked with 5% NFDM for 30 minutes, followed by four 5-minute washes with PBST.

ELISA

Gamma-Irradiated, sucrose-purified EBOV virions were coated onto 96 well, flat-bottom plates at an optimized dilution of 1:1,000. Plates were then washed and blocked with PBST + 5% NFDM. Cell lysate or serum samples were initially diluted 1:100 in PBS and subsequently

diluted 2-fold then applied to coated wells and incubated for 1 hr. Plates were then washed and incubated with HRP-conjugated goat anti-mouse secondary antibody (Promega). Next, plates were washed and ABTS substrate was added as per manufacturer's instructions (Pierce). Plates were then read on a microplate reader (Molecular Devices) and data was subsequently analyzed using Softmax pro software (Molecular Devices). Endpoint titers were determined for each sample using a cutoff of two standard deviations above the signal observed in the negative control wells.

Peptide ELISA

A library of biotinylated 18-mer peptides with a 6 amino acid overlap spanning the entire EBOV GP was constructed by Mimotopes (Raleigh, NC). These peptides served as coating antigens in our peptide ELISA. Each well of flat-bottom, 96-well assay plates was coated with a single peptide at a concentration of 2 mg/mL. Plates were then washed with PBST followed by blocking with PBST + 5% NFDM. Plates were washed again and serum samples were applied at a 1:1,000 dilution. After incubation for 1 hr, plates were washed with PBS and HRP-conjugated goat anti-mouse secondary antibody (Promega) was applied and incubated for 1 hr. Finally, plates were washed with PBST, developed using ABTS substrate as per manufacturer's instructions (Pierce), and read on a microplate reader (Molecular Devices).

Acknowledgements

Research was conducted under an IACUC approved protocol in compliance with the Animal Welfare Act, PHS Policy, and other Federal statutes and regulations relating to animals and experiments involving animals. The facility where this research was conducted is accredited by the Association for Assessment and Accreditation of Laboratory Animal Care, International and

adheres to principles stated in the Guide for the Care and Use of Laboratory Animals, National Research Council, 2011. Support for this research was provided by the Joint Science and Technology Office of the Defense Threat Reduction Agency, the Military Infectious Diseases Research Program of the United States (US) Army Medical Research and Materiel Command and the US Department of Defense (DoD) High-Performance Computing Modernization Program. These studies were performed while DM held a National Research Council Postdoctoral Fellowship at USAMRIID. The opinions, interpretations, conclusions, and recommendations contained herein are those of the authors and are not necessarily endorsed by the U.S. Army.

References

1. Grant-Klein RJ, Altamura LA, Badger CV, Bounds CE, Van Deusen NM, Kwilas SA, et al. Codon-optimized filovirus DNA vaccines delivered by intramuscular electroporation protect cynomolgus macaques from lethal Ebola and Marburg virus challenges. Human vaccines & immunotherapeutics 2015; 11:1991-2004.
2. Grant-Klein RJ, Van Deusen NM, Badger CV, Hannaman D, Dupuy LC, Schmaljohn CS. A multiagent filovirus DNA vaccine delivered by intramuscular electroporation completely protects mice from ebola and Marburg virus challenge. Human vaccines & immunotherapeutics 2012; 8:1703-6.
3. Mellquist-Riemenschneider JL, Garrison AR, Geisbert JB, Saikh KU, Heidebrink KD, Jahrling PB, et al. Comparison of the protective efficacy of DNA and baculovirus-derived protein vaccines for EBOLA virus in guinea pigs. Virus research 2003; 92:187-93.
4. Corti D, Voss J, Gamblin SJ, Codoni G, Macagno A, Jarrossay D, et al. A neutralizing antibody selected from plasma cells that binds to group 1 and group 2 influenza A hemagglutinins. Science 2011; 333:850-6.
5. Timmerman P, Puijk WC, Meloen RH. Functional reconstruction and synthetic mimicry of a conformational epitope using CLIPS technology. Journal of molecular recognition : JMR 2007; 20:283-99.
6. Wilson JA, Hevey M, Bakken R, Guest S, Bray M, Schmaljohn AL, et al. Epitopes involved in antibody-mediated protection from Ebola virus. Science 2000; 287:1664-6.

7. Dube D, Brecher MB, Delos SE, Rose SC, Park EW, Schornberg KL, et al. The primed ebolavirus glycoprotein (19-kilodalton GP1,2): sequence and residues critical for host cell binding. Journal of virology 2009; 83:2883-91.

8. Schornberg K, Matsuyama S, Kabsch K, Delos S, Bouton A, White J. Role of endosomal cathepsins in entry mediated by the Ebola virus glycoprotein. Journal of virology 2006; 80:4174-8.

9. Chandran K, Sullivan NJ, Felbor U, Whelan SP, Cunningham JM. Endosomal proteolysis of the Ebola virus glycoprotein is necessary for infection. Science 2005; 308:1643-5.

10. Kugelman JR, Kugelman-Tonos J, Ladner JT, Pettit J, Keeton CM, Nagle ER, et al. Emergence of Ebola Virus Escape Variants in Infected Nonhuman Primates Treated with the MB-003 Antibody Cocktail. Cell reports 2015; 12:2111-20.

11. Olal D, Kuehne AI, Bale S, Halfmann P, Hashiguchi T, Fusco ML, et al. Structure of an antibody in complex with its mucin domain linear epitope that is protective against Ebola virus. Journal of virology 2012; 86:2809-16.

12. Dowling W, Thompson E, Badger C, Mellquist JL, Garrison AR, Smith JM, et al. Influences of glycosylation on antigenicity, immunogenicity, and protective efficacy of ebola virus GP DNA vaccines. Journal of virology 2007; 81:1821-37.

13. Warfield KL, Swenson DL, Olinger GG, Nichols DK, Pratt WD, Blouch R, et al. Gene-specific countermeasures against Ebola virus based on antisense phosphorodiamidate morpholino oligomers. PLoS pathogens 2006; 2:e1.

14. Geisbert TW, Hensley LE, Jahrling PB, Larsen T, Geisbert JB, Paragas J, et al. Treatment of Ebola virus infection with a recombinant inhibitor of factor VIIa/tissue factor: a study in rhesus monkeys. Lancet 2003; 362:1953-8.

15. Lee JE, Fusco ML, Hessell AJ, Oswald WB, Burton DR, Saphire EO. Structure of the Ebola virus glycoprotein bound to an antibody from a human survivor. Nature 2008; 454:177-82.

16. Davidson E, Bryan C, Fong RH, Barnes T, Pfaff JM, Mabila M, et al. Mechanism of Binding to Ebola Virus Glycoprotein by the ZMapp, ZMAb, and MB-003 Cocktail Antibodies. Journal of virology 2015; 89:10982-92.

17. Murin CD, Fusco ML, Bornholdt ZA, Qiu X, Olinger GG, Zeitlin L, et al. Structures of protective antibodies reveal sites of vulnerability on Ebola virus. Proceedings of the National Academy of Sciences of the United States of America 2014; 111:17182-7.

18. Tran EE, Nelson EA, Bonagiri P, Simmons JA, Shoemaker CJ, Schmaljohn CS, et al. Mapping of Ebolavirus Neutralization by Monoclonal Antibodies in the ZMapp Cocktail Using Cryo-Electron Tomography and Studies of Cellular Entry. Journal of virology 2016; 90:7618-27.

19. Pallesen J, Murin CD, de Val N, Cottrell CA, Hastie KM, Turner HL, et al. Structures of Ebola virus GP and sGP in complex with therapeutic antibodies. Nature microbiology 2016; 1:16128.

20. Schmaljohn C, Vanderzanden L, Bray M, Custer D, Meyer B, Li D, et al. Naked DNA vaccines expressing the prM and E genes of Russian spring summer encephalitis virus and Central European encephalitis virus protect mice from homologous and heterologous challenge. Journal of virology 1997; 71:9563-9.

21. Luxembourg A, Hannaman D, Ellefsen B, Nakamura G, Bernard R. Enhancement of immune responses to an HBV DNA vaccine by electroporation. Vaccine 2006; 24:4490-3.

22. Lee JE, Kuehne A, Abelson DM, Fusco ML, Hart MK, Saphire EO. Complex of a protective antibody with its Ebola virus GP peptide epitope: unusual features of a V lambda x light chain. Journal of molecular biology 2008; 375:202-16.

Figure Legends

Figure 1. Antibody binding after full substitution mutagenesis of $_{391}$TPVYKLDISEATQVEQHHRRTDNDS$_{415}$. Substituted amino acids are shown on the right side of each heat map. Green indicates significantly reduced binding **(A)** The core of the mAb 13F6 epitope was determined to be $_{406}$QHHRRTD$_{412}$, with $_{406}$QXXRXT$_{411}$ being most essential for binding. **(B)** The core of mAb 6E3 was also $_{406}$QHHRRTD$_{412}$, with $_{406}$QXHRR$_{410}$ most essential to binding. **(C)** The core of the epitope for mAb 6D8 was determined to be $_{394}$YKLDI$_{398}$, with $_{395}$KLD$_{397}$ as the most essential amino acids**. (D)** Polyclonal sera from mice vaccinated with WT GP of EBOV showed strongest binding to $_{397}$DISEAT$_{402}$, with $_{398}$ISXXT$_{402}$ as the most crucial amino acids.

Figure 2. Full substitution mutagenesis of mAbs 13C6 and 6D8. **(A)** Binding of mAb 6D8 to a full series of substitutions of $_{391}$TPVYKLDISEATQVEQHHRRTDNDS$_{415}$ indicates decreased binding upon mutations to $_{393}$VYKLD$_{397}$ (boxed), which is thought to be the epitope core. **(B)** Binding of mAb 6D8 to a full substitution series of $_{470}$GEESASSGKLGLITNTIAGVAGLIT$_{493}$ indicates no binding to this stretch of amino acids. **(C)** Binding of mAb 13C6 to a full substitution series of $_{470}$GEESASSGKLGLITNTIAGVAGLIT$_{493}$ indicates decreased binding upon mutations to $_{487}$GVAGLIT$_{493}$ (boxed) and appears to be generally sensitive to introduction of negative charges into the peptides. **(D)** Binding of mAb 13C6 to a full substitution series of $_{391}$TPVYKLDISEATQVEQHHRRTDNDS$_{415}$ indicates no binding to this stretch of amino acids.

Figure 3. Relative binding of serum samples from mice, guinea pigs and rhesus macaques to amino acids in CLIPS. Blue indicates strong binding and tan indicates weaker binding. No color indicates no measureable binding with that particular sample.

Figure 4. EBOV GP structural modeling. A surface model representation of the EBOV GP trimer is shown in white. The 3D representation omits the mucin-like domain in GP, which is considered unstructured. Smooth regions of the surface highlight the parts of the structure that were determined through x-ray crystallography [22]. Other portions of the structure that were not resolved experimentally have been modelled "de novo" and are shown as collections of dots to indicate the approximate location of the missing fragments. Epitopes M1 to M4 identified in the CLIPS study and included in the multi-epitope constructs described in Table 1 are highlighted in purple, blue, magenta and red, respectively.

Figure 6. Mep 1 and Mep2 expression. **(A)** Cells were transfected with the Mep1 or Mep2 DNA vaccine constructs or with the WT GP DNA vaccine and stained with DAPI (top panels). Immunofluorescent antibody staining was performed with EBOV mouse mAb 6D8 (middle panels). Lower panels show a merge of the top and middle panels. **(B)** ELISA was performed on cell supernatants of mock-transfected cells or cells transfected with the Mep1 or Mep2 constructs. **(C)** Groups of mice (*N* = 10) were vaccinated three times with empty plasmid vector, the WT GP DNA vaccine, or the Mep1 or Mep2 constructs. ELISA was performed on serum samples obtained 3 weeks after each vaccination using inactivated EBOV virions as antigen.

Table 1. Predicted features and amino acid compositions of expression products encoded by the Mep1 and Mep2 DNA vaccines

Mep1				
Epitope	**Predicted Features**	**Predicted Amino Acid Sequence**	**Linker**	**Amino Acids**
SP	Signal peptide	MGVTGILQLPRDRFKRTSFFLWVIILFQRTFSI	None	1-33
M1	Linear- Accessible	FRSGVPPK	GGGG	88-95
M2	Linear- Accessible	LEIKKPDG	GGGG	111-118
mAb 6D8	Linear- mucin	PVYKLDISEA	GGGG	392-401
mAb 13F6	Linear- mucin	QHHRRT	GGGG	406-411
mAb 12B5 (partial)	Linear- mucin	GKLGLITN	GGGG	477-484
TM	Transmembrane domain	WIPAGIGVTGVIIAVIALFCICKFVF	None	651-676
Mep2				
Epitope	**Predicted Features**	**Predicted Amino Acid Sequence**	**Linker**	**Amino Acids**
SP-GP1	Signal peptide	MGVTGILQLPRDRFKRTSFFLWVIILFQRTFSI - PLGVIHN	GGGG	1-40
mAb 6D8	Linear- mucin	PVYKLDISEA	GGGG	392-401
mAb 13F6	Linear- mucin	QHHRRT	GGGG	406-411
mAb 12B5 (partial)	Linear- mucin	GKLGLITN	GGGG	477-484
M3	Linear	VSDVDKLVCRDKL	GGGG	45-57
M4	Linear	SSHPLREPV	GGGG	195-203
Conf-1	Conformational-mucin	CTPVYKLDISCCENTNTSKGTC	GGGG	391-399_433-441
Conf-2	Conformational-mucin	CTPVYKLDISCCAGPPKAENTC	GGGG	91-399_427-435

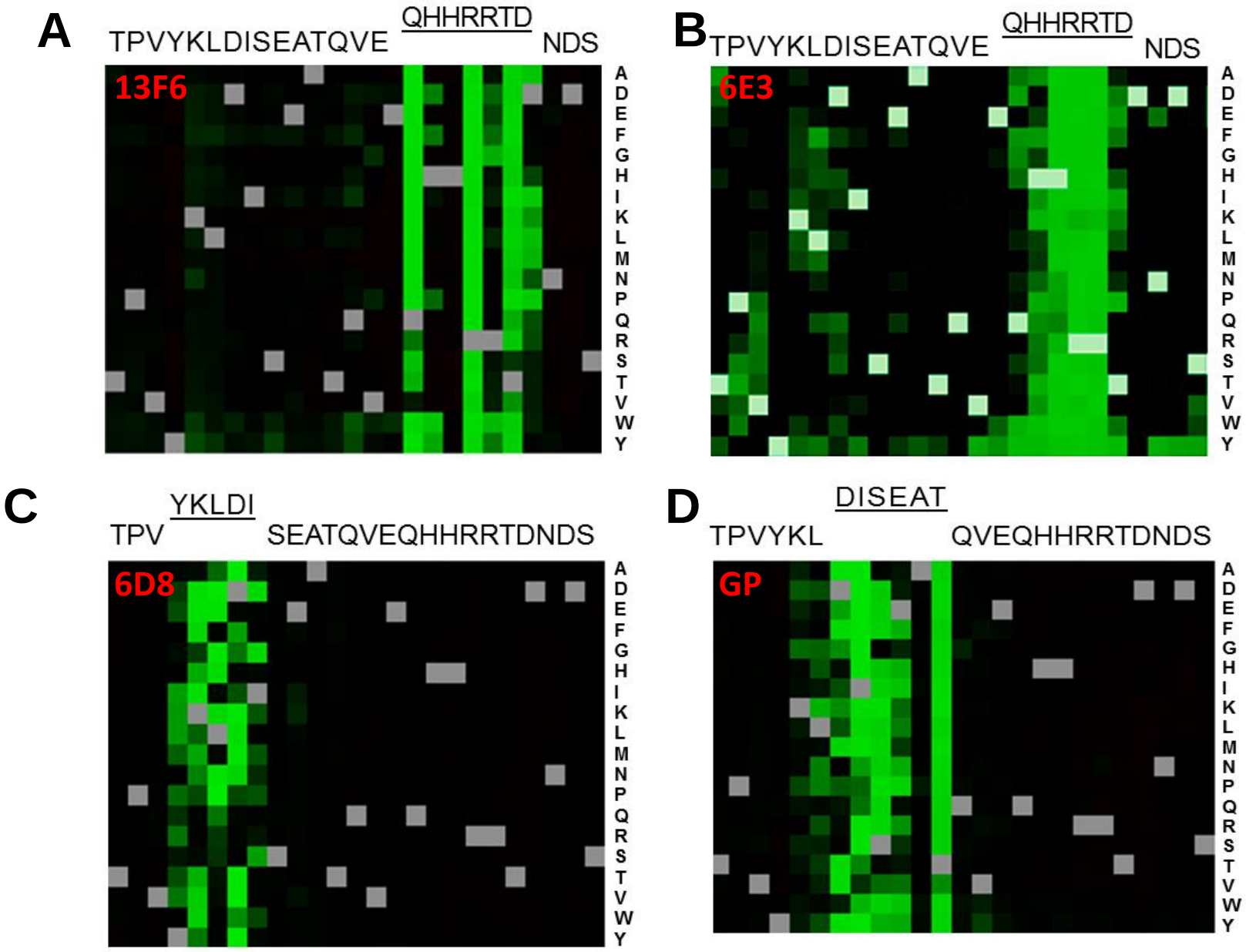
A
TPVYKLDISEATQVE
QHHRRTD
NDS
13F6
A D E F G H I K L M N P Q R S T V W Y
B
TPVYKLDISEATQVE
QHHRRTD
NDS
6E3
A D E F G H I K L M N P Q R S T V W Y
C
TPV
YKLDI
SEATQVEQHHRRTDNDS
6D8
A D E F G H I K L M N P Q R S T V W Y
D
TPVYKL
DISEAT
QVEQHHRRTDNDS
GP
A D E F G H I K L M N P Q R S T V W Y

Figure 1

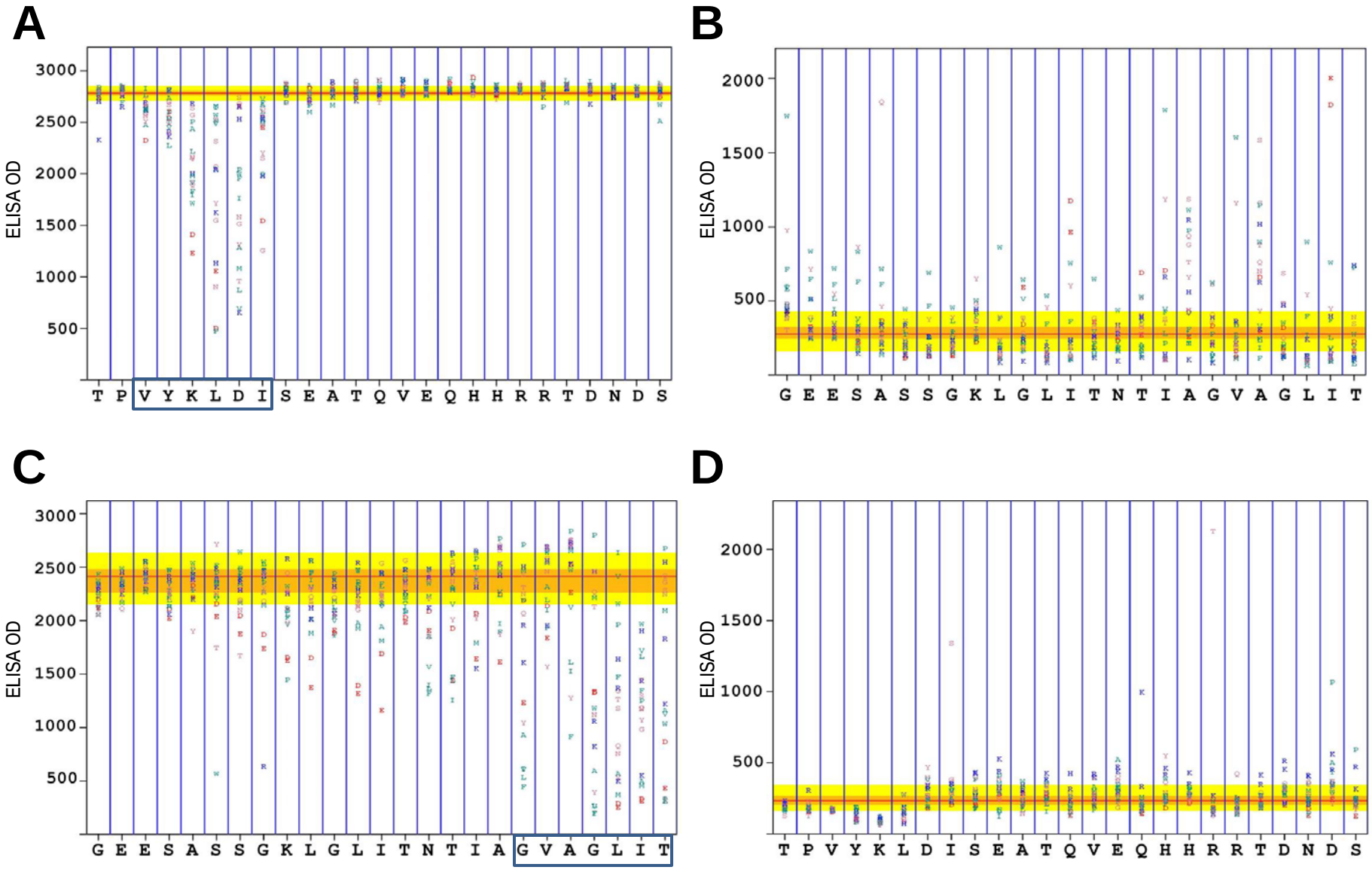
A
ELISA OD
3000
2500
2000
1500
1000
500
T P V Y K L D I S E A T Q V E Q H H R R T D N D S
B
ELISA OD
2000
1500
1000
500
G E E S A S S G K L G L I T N T I A G V A G L I T
C
ELISA OD
3000
2500
2000
1500
1000
500
G E E S A S S G K L G L I T N T I A G V A G L I T
D
ELISA OD
2000
1500
1000
500
T P V Y K L D I S E A T Q V E Q H H R R T D N D S

Figure 2

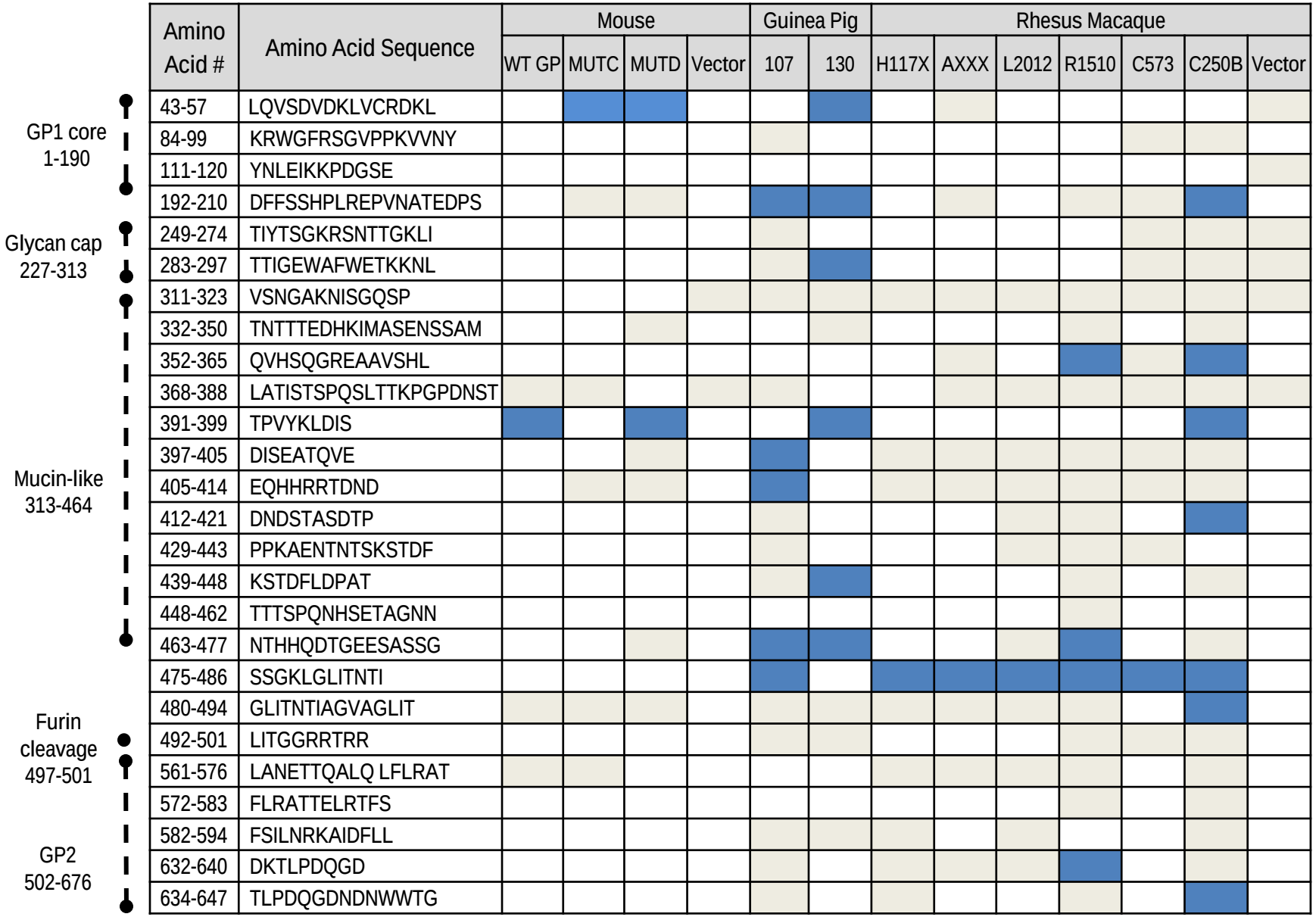

Amino Acid #	Amino Acid Sequence	Mouse				Guinea Pig		Rhesus Macaque						
		WT GP	MUTC	MUTD	Vector	107	130	H117X	AXXX	L2012	R1510	C573	C250B	Vector
43-57	LQVSDVDKLVCRDKL													
84-99	KRWGFRSGVPPKVVNY													
111-120	YNLEIKKPDGSE													
192-210	DFFSSHPLREPVNATEDPS													
249-274	TIYTSGKRSNTTGKLI													
283-297	TTIGEWAFWETKKNL													
311-323	VSNGAKNISGQSP													
332-350	TNTTTEDHKIMASENSSAM													
352-365	QVHSQGREAAVSHL													
368-388	LATISTSPQSLTTKPGPDNST													
391-399	TPVYKLDIS													
397-405	DISEATQVE													
405-414	EQHHRRTDND													
412-421	DNDSTASDTP													
429-443	PPKAENTNTSKSTDF													
439-448	KSTDFLDPAT													
448-462	TTTSPQNHSETAGNN													
463-477	NTHHQDTGEESASSG													
475-486	SSGKLGLITNTI													
480-494	GLITNTIAGVAGLIT													
492-501	LITGGRRTRR													
561-576	LANETTQALQ LFLRAT													
572-583	FLRATTELRTFS													
582-594	FSILNRKAIDFLL													
632-640	DKTLPDQGD													
634-647	TLPDQGDNDNWWTG													

Figure 3

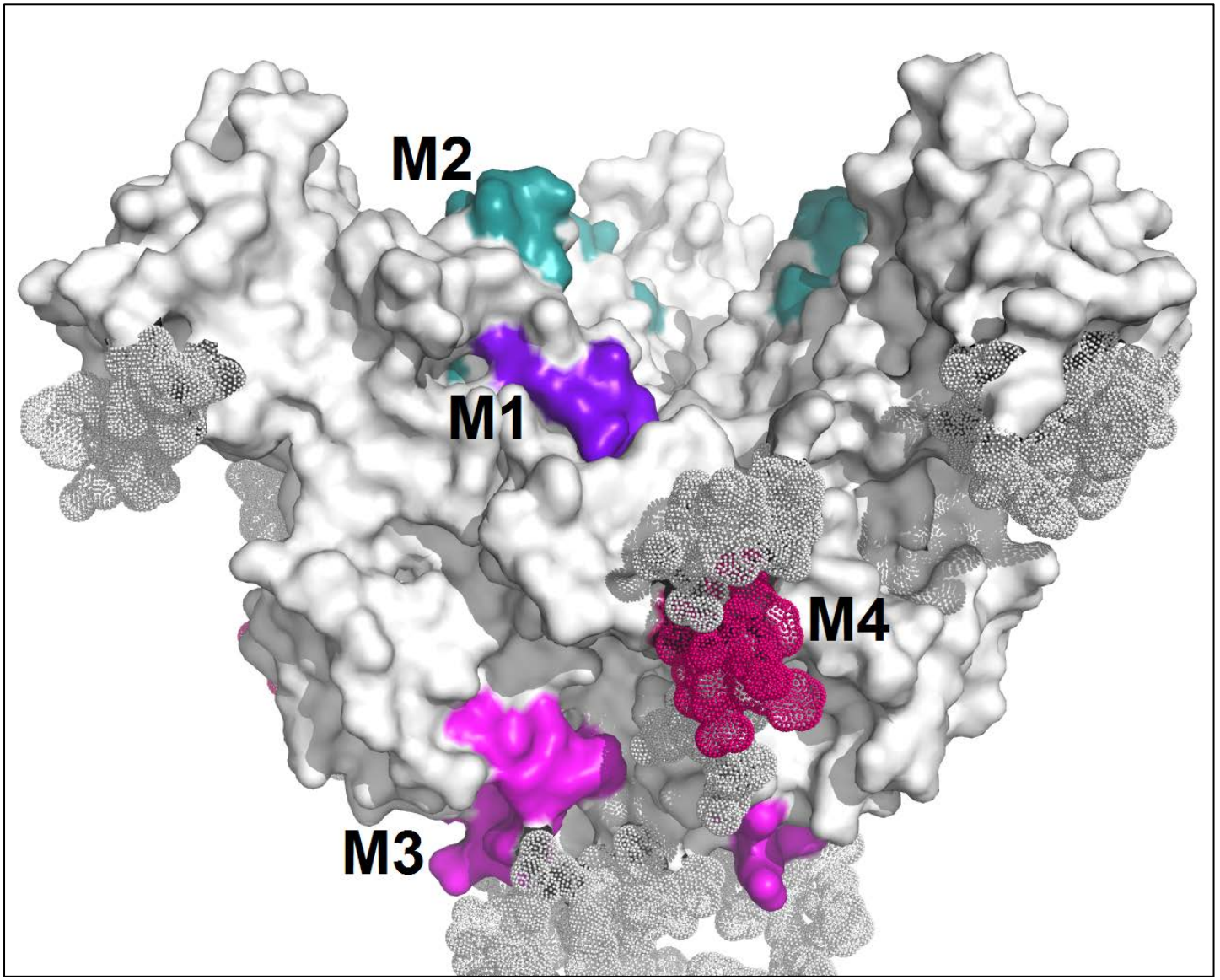

Figure 4

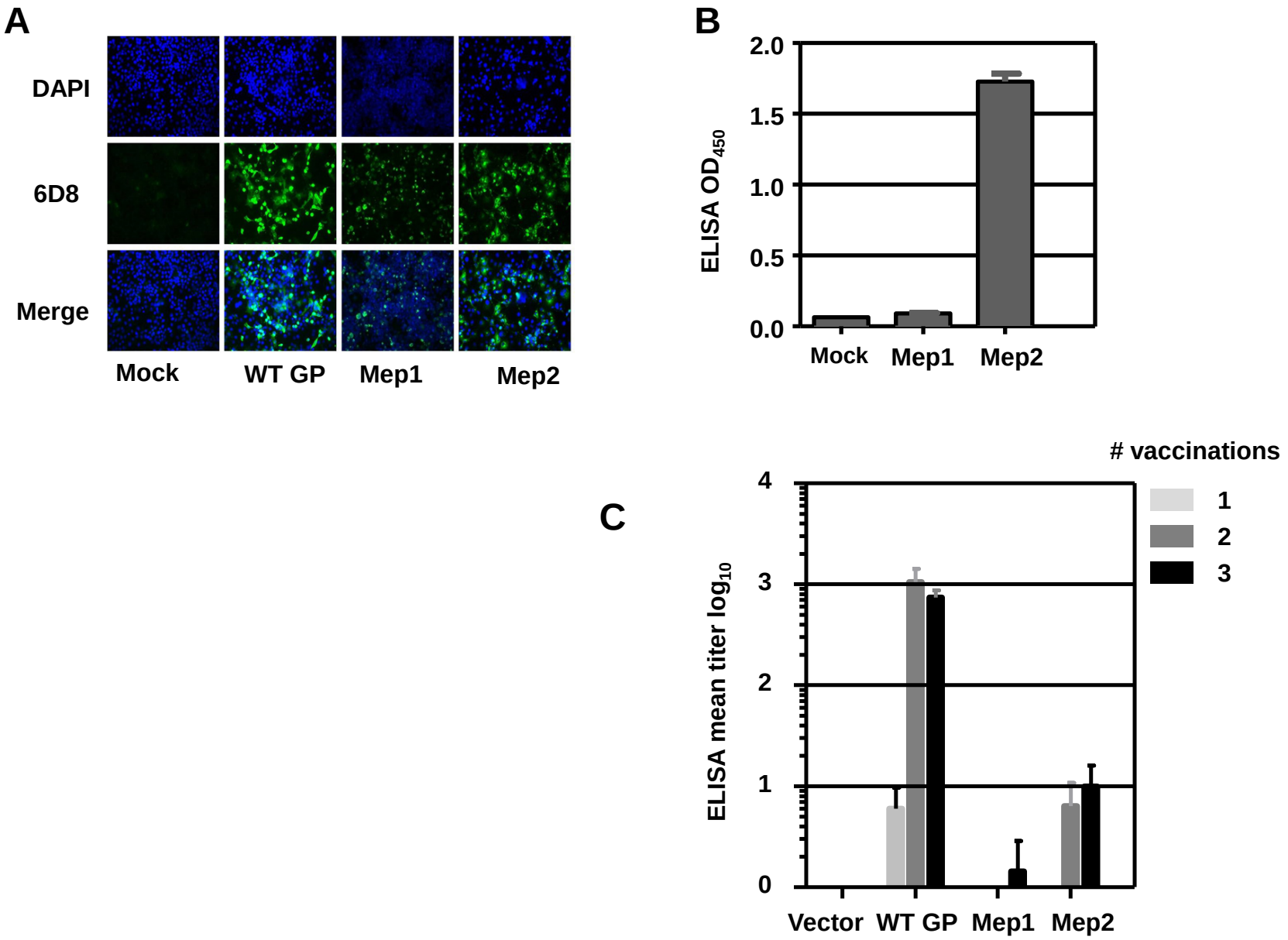
A
DAPI
6D8
Merge
Mock
WT GP
Mep1
Mep2
B
ELISA OD450
2.0
1.5
1.0
0.5
0.0
Mock
Mep1
Mep2
C
vaccinations
1
2
3
ELISA mean titer log10
4
3
2
1
0
Vector
WT GP
Mep1
Mep2

Figure 5

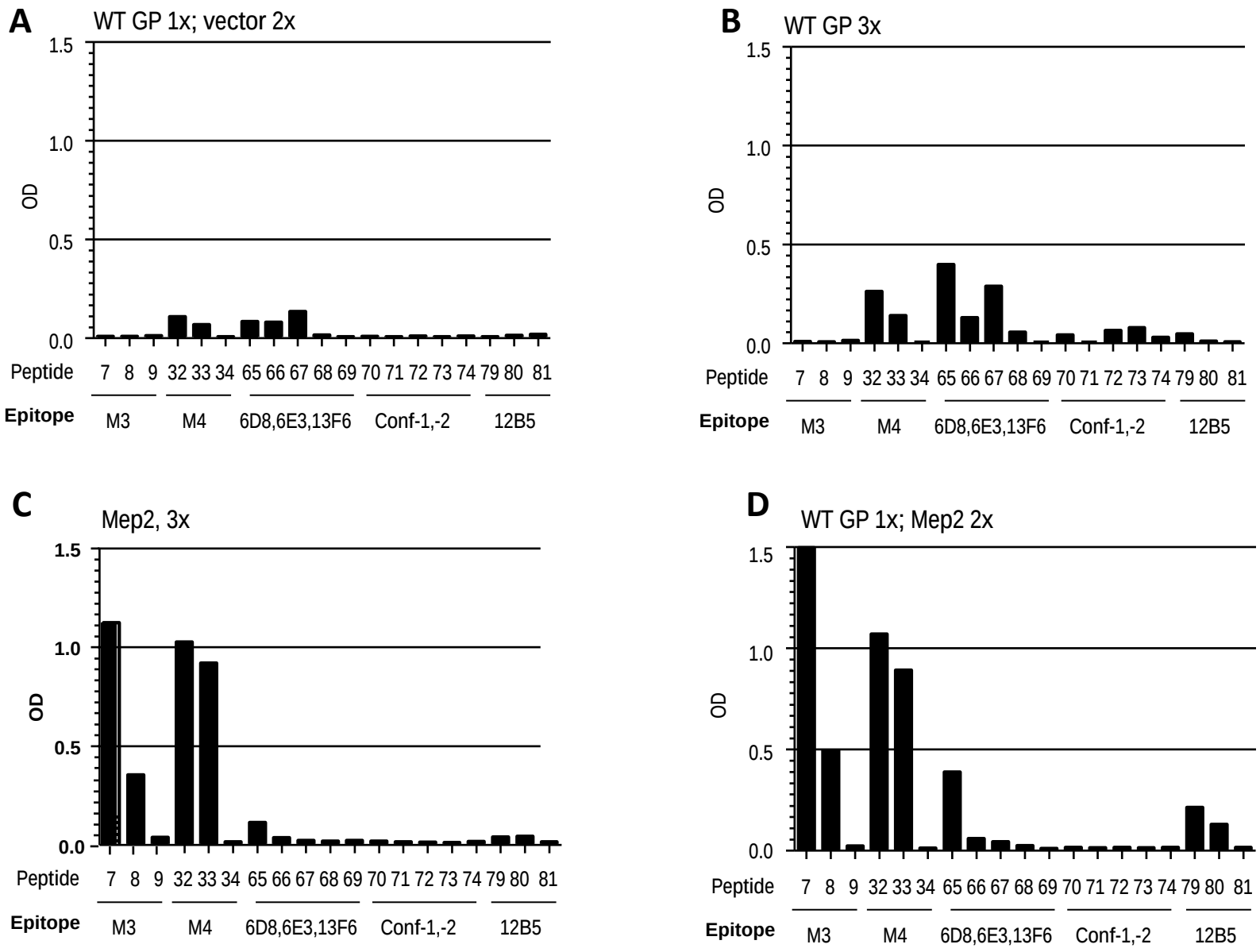
A
WT GP 1x; vector 2x
B
WT GP 3x
C
Mep2, 3x
D
WT GP 1x; Mep2 2x
OD
1.5
1.0
0.5
0.0
Peptide
7 8 9 32 33 34 65 66 67 68 69 70 71 72 73 74 79 80 81
Epitope
M3
M4
6D8,6E3,13F6
Conf-1,-2
12B5

Figure 6

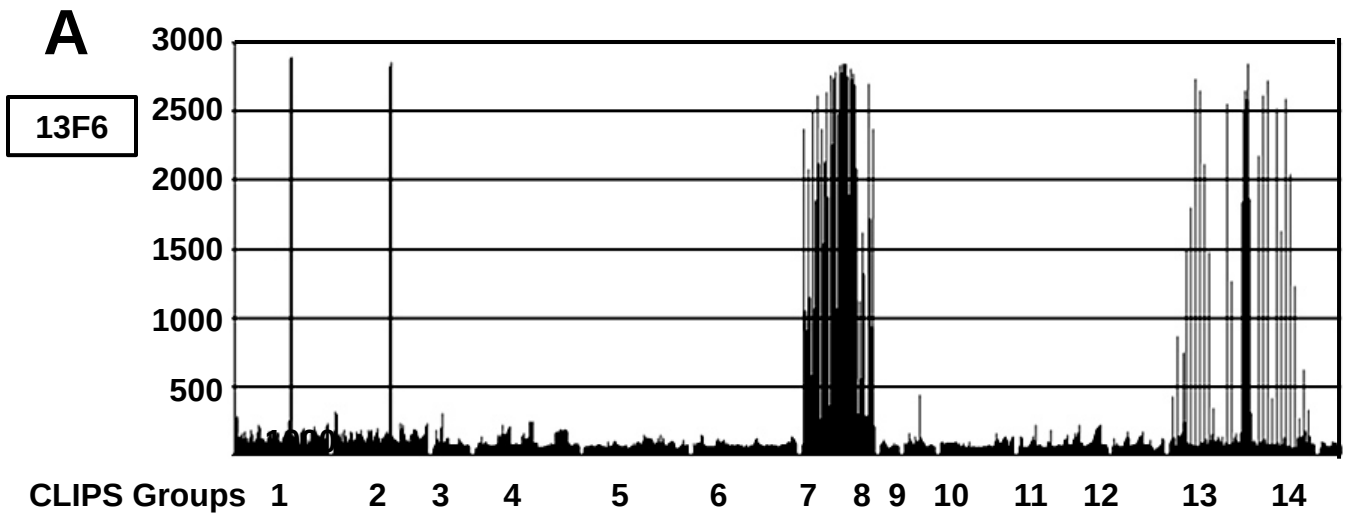

B

Group-1

```
    CATQVEQHHRRTDNDSC
     CTQVEQHHRRTDNDSTC
 CISEATQVEQHHRRTDC
      CQVEQHHRRTDNDSTAC
        CEQHHRRTDNDSTASDC
   CEATQVEQHHRRTDNDC
  CSEATQVEQHHRRTDNC
       CVEQHHRRTDNDSTASC
         CQHHRRTDNDSTASDTC
CDISEATQVEQHHRRTC
```

Group-7

```
1CSSGKLGLIT1TTKPGPDNSCQVEQHHRRT1
1CGTNTTTEDH1QVEQHHRRTCQVEQHHRRT1
1CSFTVVSNGA1SPQNHSETACQVEQHHRRT1
1CSSGKLGLIT1AGPPKAENTCQVEQHHRRT1
1CQVEQHHRRT1GTNTTTEDHCQVEQHHRRT1
1CTTKPGPDNS1AGPPKAENTCQVEQHHRRT1
1CSPQNHSETA1TTKPGPDNSCQVEQHHRRT1
1CSQGREAAVS1AGPPKAENTCQVEQHHRRT1
1CSPQNHSETA1AGPPKAENTCQVEQHHRRT1
1CAGPPKAENT1AGPPKAENTCQVEQHHRRT1
```

Group-2

```
      TQVEQHHRRTDNDST
         EQHHRRTDNDSTASD
          QHHRRTDNDSTASDT
  ISEATQVEQHHRRTD
    ATQVEQHHRRTDNDS
  SEATQVEQHHRRTDN
   EATQVEQHHRRTDND
      QVEQHHRRTDNDSTA
 DISEATQVEQHHRRT
LDISEATQVEQHHRR
```

Group-13

```
       CAMVQVHSQGCRRTDNDSTAC
            CQVEQHHRRTCEDHKIMASEC
            CQVEQHHRRTCENTNTSKSTC
CAGPPKAENTCQVEQHHRRTC
            CQVEQHHRRTCASENSSAMVC
            CQVEQHHRRTCAGPPKAENTC
            CQVEQHHRRTCETAGNNNTHC
CTGEESASSGCQVEQHHRRTC
            CQVEQHHRRTCTTKPGPDNSC
CDNSTHNTPVCQVEQHHRRTC
```

Figure S1

A

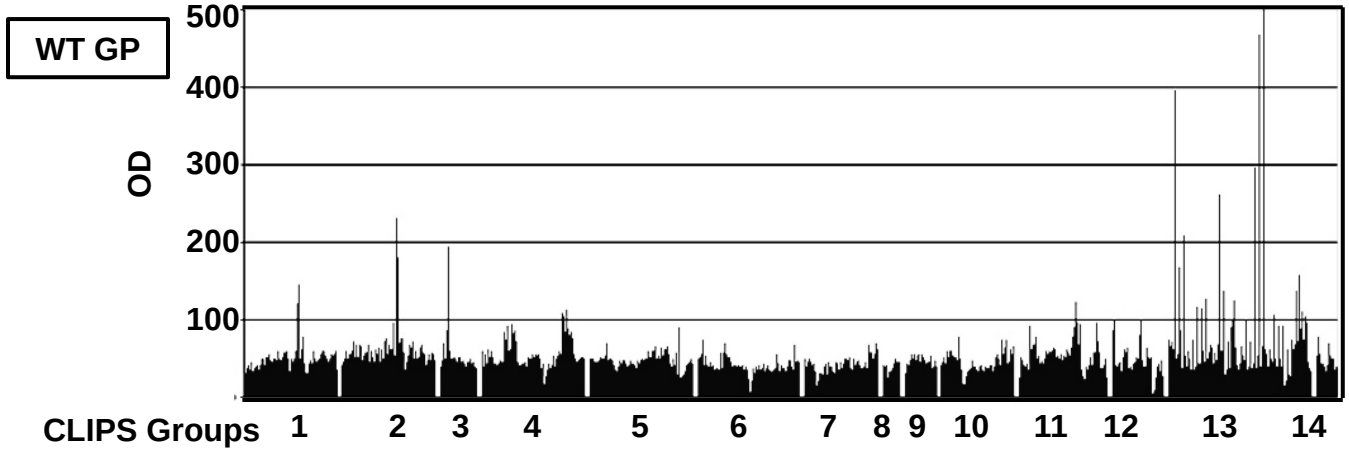

B

Group-1

```
            CYKLDISEATQVEQHHC   144
         CNTPVYKLDISEATQVC      136
            CVYKLDISEATQVEQHC   128
          CTPVYKLDISEATQVEC     125
    CDNSTHNTPVYKLDISC           120
   CPDNSTHNTPVYKLDIC            115
       CTHNTPVYKLDISEATC        111
      CSTHNTPVYKLDISEAC         087
     CNSTHNTPVYKLDISEC          083
           CPVYKLDISEATQVEQC    081
CKPGPDNSTHNTPVYKC               075
  CGPDNSTHNTPVYKLDC             074
        CHNTPVYKLDISEATQC       065
 CPGPDNSTHNTPVYKLC              062

        CTAAGPPKAENTNTSKC       077
```

Group-2

```
GPDNSTHNTPVYKLD                 230
  DNSTHNTPVYKLDIS               150
 PDNSTHNTPVYKLDI                147
           YKLDISEATQVEQHH       179
       HNTPVYKLDISEATQ           152
  DNSTHNTPVYKLDIS               150
 PDNSTHNTPVYKLDI                147
           VYKLDISEATQVEQH       127
          PVYKLDISEATQVEQ        120
        NTPVYKLDISEATQV          119
         TPVYKLDISEATQVE         113
      THNTPVYKLDISEAT           093
     STHNTPVYKLDISEA            088
    NSTHNTPVYKLDISE             085


   LATISTSPQSLTTKP              096
    TISTSPQSLTTKPGP             089
   ATISTSPQSLTTKPG              084
```

Group-13

```
           CTPVYKLDISCENTNTSKSTC         822
           CTPVYKLDISCAGPPKAENTC         467
           CTPVYKLDISCNGAKNISGQC         396
           CTPVYKLDISCPSATTAAGPC         296
           CTPVYKLDISCTSPQSLTTKC         262
           CTPVYKLDISCRTSSDPGTNC         208
           CTPVYKLDISCSGQSPARTSC         168
           CTPVYKLDISCTTKPGPDNSC         137
           CTPVYKLDISCSSGKLGLITC         136
           CTPVYKLDISCSQGREAAVSC         126
CENTNTSKSTCTPVYKLDISC                    124
           CTPVYKLDISCASENSSAMVC         116
           CTPVYKLDISCAMVQVHSQGC         115
           CTPVYKLDISCDPATTTSPQC         107
           CTPVYKLDISCAGVAGLITGC         104
CAGPPKAENTCTPVYKLDISC                    102
           CTPVYKLDISCRRTDNDSTAC         101

            CTSPQSLTTKCLITNTIAGVC        157
            CAGVAGLITGCLITNTIAGVC        111
                     CLITNTIAGVCLITNTIAGVC106
            CSSGKLGLITCLITNTIAGVC        103
            CAVSHLTTLACLITNTIAGVC        100
```

Group-3

```
1ELRTFSILN1TQALQLFLR1   193
1RWGGTAHIL1TQALQLFLR1   172
1ILNRKAIDF1TQALQLFLR1   169
1FLRATTELR1TQALQLFLR1   128
1IDFLLQRWG1TQALQLFLR1   119
```

Figure S2

A

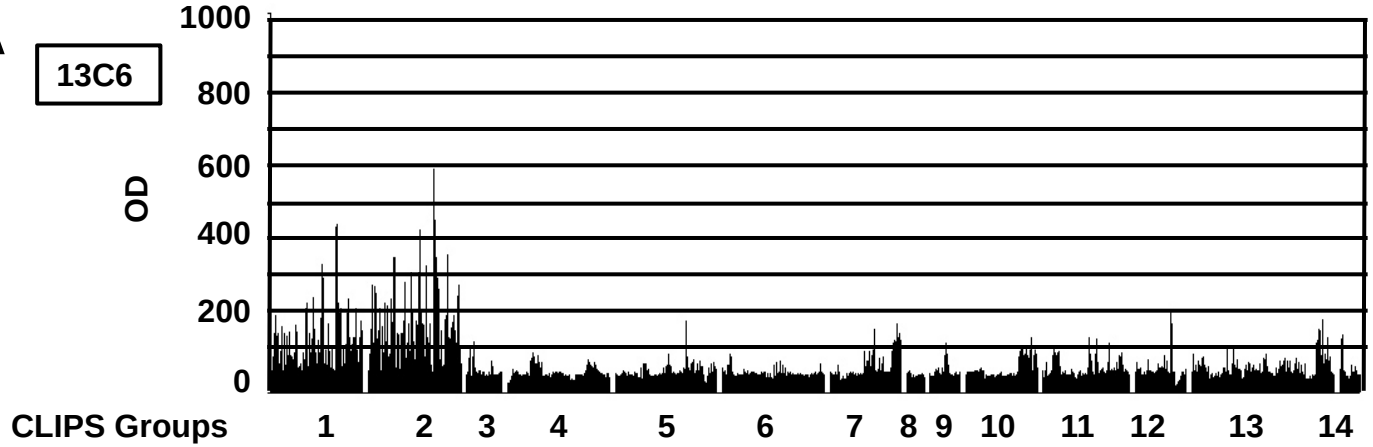

B

Group-1

```
        CGKLGLITNTIAGVAGC
   CESASSGKLGLITNTIC
     CASSGKLGLITNTIAGC
    CSASSGKLGLITNTIAC
         CKLGLITNTIAGVAGLC
      CSSGKLGLITNTIAGVC
       CSGKLGLITNTIAGVAC
  CEESASSGKLGLITNTC
CTGEESASSGKLGLITC

     CLATISTSPQSLTTKPC
```

Group-2

```
    ESASSGKLGLITNTI
 TGEESASSGKLGLIT
            GLITNTIAGVAGLIT
        SSGKLGLITNTIAGV
          GKLGLITNTIAGVAG
        SGKLGLITNTIAGVA
DTGEESASSGKLGLI
  GEESASSGKLGLITN
      ASSGKLGLITNTIAG
          KLGLITNTIAGVAGL

       TISTSPQSLTTKPGP
     LATISTSPQSLTTKP
   TTLATISTSPQSLT
```

Group-7

```
1CAGPPKAENT1TTKPGPDNSCSSGKLGLIT1
          1CSPQNHSETA1SSGKLGLITCQVEQHHRRT1
1CSSGKLGLIT1AGPPKAENTCSSGKLGLIT1
1CSPQNHSETA1AGPPKAENTCSSGKLGLIT1
1CSSGKLGLIT1TTKPGPDNSCSSGKLGLIT1
```

Group-12

```
CREPVNATEDCRSNTTGKLIC
CTIGEWAFWECRSNTTGKLIC
CNPEIDTTIGCRSNTTGKLIC
CGFGTNETEYCRSNTTGKLIC
CIRYQATGFGCRSNTTGKLIC
CTEYLFEVDNCRSNTTGKLIC
```

Group-13

```
      CTSPQSLTTKCLITNTIAGVC
CDNSTHNTPVCSSGKLGLITC
CETAGNNNTHCSSGKLGLITC
CDPATTTSPQCSSGKLGLITC
CSTASDTPSACSSGKLGLITC
 CTSPQSLTTKCAGVAGLITGC
```

Figure S3

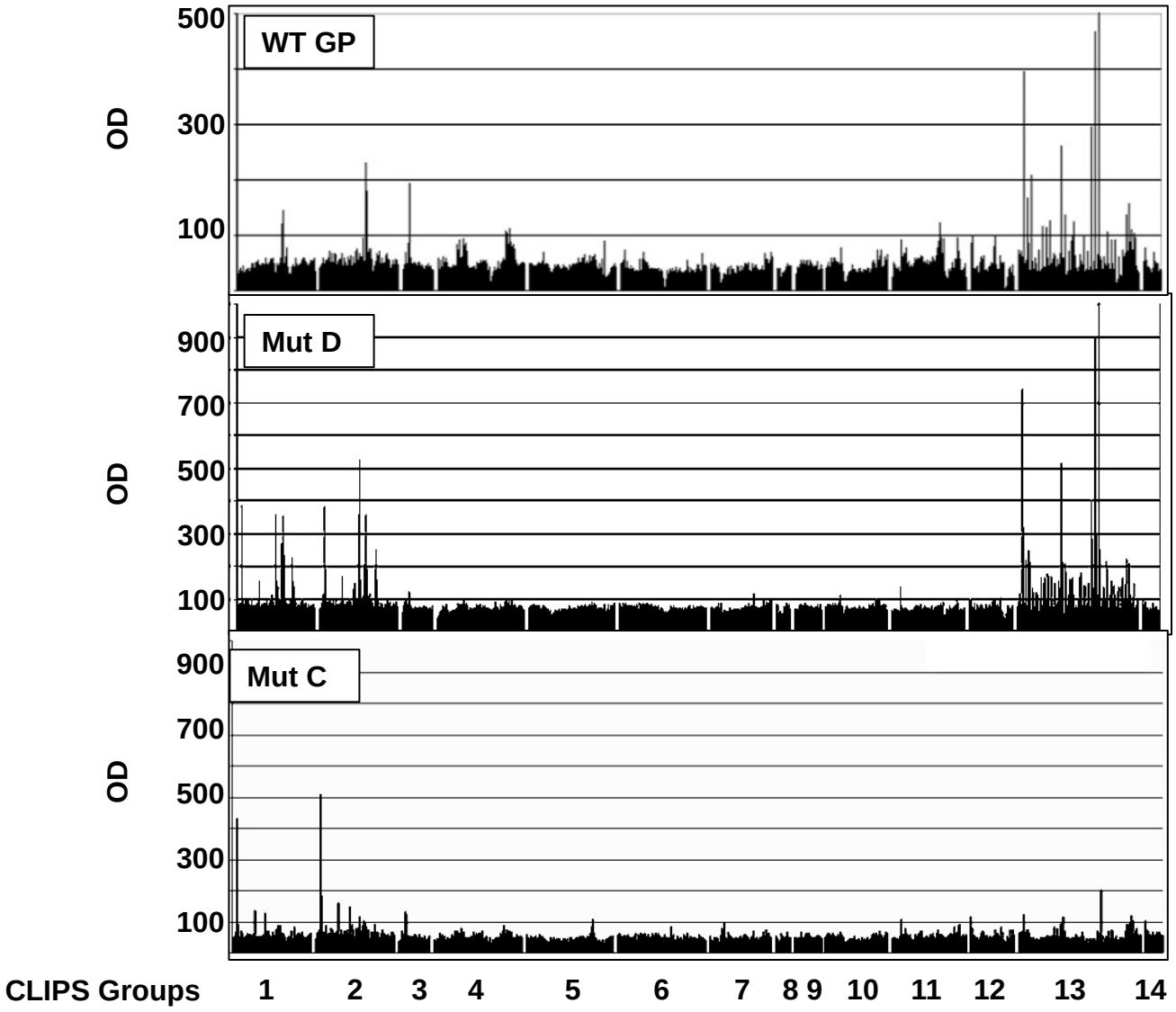
WT GP
Mut D
Mut C
OD
500
300
100
900
700
500
300
100
900
700
500
300
100
CLIPS Groups
1
2
3
4
5
6
7
8
9
10
11
12
13
14

Figure S4

Table S1. Peptides used in ELISA to assess Mep2 responses*

Peptide Sequence	Peptide #	Epitope(s)
VIHNSTLQ**VSDVDKLVCR**	7	M3
LQ**VSDVDKLVCRDKL**SST	8	
DKLVCRDKLSSTNQLRSV	9	
PQAKKDFF**SSHPLREPV**N	32	M4
FF**SSHPLREPV**NATEDPS	33	
LREPVNATEDPSSGYYST	34	
DNSTHNT**PVYKLDISEA**T	65	6D8, 6E3, 13F6
T**PVYKLDISEA**TQVE**QHH**	66	
DISEATQVE**QHHRRT**DND	67	
QVE**QHHRRT**DNDSTASDT	68	
RRTDNDSTASDTPPATTA	69	
STASDTPPATTA**AGPLKA**	70	Conf-1 and Conf-2
PPATTA**AGPLKAENTNTS**	71	
AGPLKAENTNTSKGTDLL	72	
ENTNTSKGTDLLDPATTT	73	
KGTDLLDPATTTSPQNHS	74	
TGEESASS**GKLGLITNT**I	79	Partial 12B5
SS**GKLGLITNT**IAGVAGL	80	
LITNTIAGVAGLITGGRR	81	

*Peptide # corresponds to those shown in Figure 6; the amino acids corresponding to those that form part or all of the listed epitope are shown in bold; the portion of mAb 12B5 included in Mep2 is in bold and the entire 12B5 epitope is underlined in peptide 80.

Figure 6. ELISA using linear peptides containing epitopes included in Mep2. Linear peptides are as defined in **Table 1** and **Table S1**. The epitopes contained in part or in whole in each of the peptides are identified beneath the peptide numbers. **(A)** Samples from mice vaccinated once with the WT GP DNA vaccine followed by two vaccinations with an empty plasmid vector control; **(B)** samples from mice vaccinated three times with the WT GP DNA vaccine; **(C)** samples from mice vaccinated three times with the Mep2 DNA vaccine; and, **(D)** samples from mice vaccinated once with the WT GP DNA vaccine followed by two vaccinations with the Mep2 DNA vaccine.

Figure S1. Epitope mapping of mAb 13F6. **(A)** The CLIPS binding profile indicates binding to peptides in groups 1 , 2, 7, and 13. (**B)** Individual peptides in each group are shown in the boxed areas with amino acids in common shown in blue.

Figure S2. Epitope mapping of sera from mice vaccinated with WT EBOV GP DNA vaccine. **(A)** The CLIPS binding profile indicates binding to peptides in groups 1 , 2, 3, and 13. **(B)** Individual peptides in each group are shown in the boxed areas with amino acids in common shown in blue.

Figure S3. Epitope mapping of mAb 13C6. **(A)** The CLIPS binding profile indicates binding to peptides in groups 1 , 2, 7, 12, and 13. **(B)** Individual peptides in each group are shown in the boxed areas with amino acids in common shown in blue.

Figure S4. CLIPS binding profiles. CLIPS binding is shown for pooled polyclonal sera from mice vaccinated with WT GP (top panel), MUTD (middle panel), or MUTC (bottom panel) DNA vaccines.